Simultaneous Localization and Antenna Calibration

Robert Pöhlmann*, Siwei Zhang*, Emanuel Staudinger*, Armin Dammann*, Peter A. Hoeher†
*Institute of Communications and Navigation, German Aerospace Center (DLR), Oberpfaffenhofen Germany,
{robert.poehlmann, emanuel.staudinger, siwei.zhang, armin.dammann}@dlr.de
†Faculty of Engineering, University of Kiel, Kiel, Germany, ph@tf.uni-kiel.de

***Abstract*—Cooperative localization fills the gap in scenarios where global navigation satellite system (GNSS) reception is denied or impaired. Position and orientation information is then often provided based on signal round-trip time (RTT) and direction-of-arrival (DoA). Obtaining a meaningful RTT requires calibrated transceiver group delays, and accurate DoA estimation requires antenna calibration. Usually, such calibrations are performed once before operation. However, calibration parameters can change over time, e.g. due to varying temperature of RF components or reconfigurable antenna surroundings. To cope with that, we propose to estimate antenna responses and ranging biases simultaneously with positions and orientations by simultaneous localization and calibration (SLAC). We derive a SLAC algorithm based on Bayesian filtering, which is suitable for arbitrary antenna types. The algorithm is evaluated with measurement data from robotic rovers. We show, that ranging and DoA performance is improved considerably, leading to better position and orientation accuracy with SLAC.**

***Index Terms*—Angle-of-arrival, antenna array, antenna response, array signal processing, direction-of-arrival, multi-mode antenna, round-trip time**

I. Introduction

Accurate localization is required by numerous applications. Cooperative radio localization is considered, where global navigation satellite systems (GNSSs) are not available or cannot meet the requirements. Areas of application include Internet of Things (IoT), autonomous driving, 5G and 6G cellular networks, and planetary exploration by robotic multi-agent systems. In general, not only position but also orientation is of interest, e.g. to determine the heading of a car or to control a robot. Abstracting from specific applications, a cooperative network consists of two types of nodes, agents and anchors. The positions and orientations of the agents need to be estimated, while the positions of the anchors are known. Distance information is obtained from the signal round-trip time (RTT), whereas direction information in terms of the direction-of-arrival (DoA) is obtained from multiport antennas like phased arrays, co-located antennas or multi-mode antennas (MMAs) [1]. Together, RTT and DoA can be used to estimate the positions and orientations of the agents.

To obtain a meaningful RTT, the group delays in the transmit and receive chains of the transceivers need to be calibrated. Accurate DoA estimation requires antenna calibration, e.g. in a dedicated measurement chamber. Such calibrations are usually performed before the system becomes operational. However, especially in commercial off-the-shelf (COTS) hardware, transceiver group delays may vary, e.g. due to temperature changes. Varying transceiver group delays result in ranging biases. For cost and practicability reasons, antennas are often calibrated in near-field measurement chambers, where only the antenna itself can be measured. When the antenna is installed in its final position, the antenna response will be different due to the influence of the surrounding structure or mounting platform, which leads to impaired DoA estimation performance. When an additional sensor is available, the true antenna response can be estimated by in-situ calibration [2]. However, without additional sensors or when the surroundings of the antenna are reconfigurable, e.g. a manipulator arm on a robot, antenna calibration must be performed during operation.

Calibration during operation is called simultaneous localization and calibration (SLAC), and is often considered as part of simultaneous localization and mapping (SLAM) [3]. An example can be found in [4], where electromagnetic distortions are calibrated to enable electromagnetic localization of instruments in a patient's body during surgery. In [5], ranging bias calibration in a non-cooperative sensor network is proposed. Calibrating the uniform linear array (ULA) of an automotive radar using targets of opportunity is also known [6], but the approach is limited to amplitude and phase calibration, neglecting other antenna response deviations. Antenna response calibration of arbitrary multiport antennas by SLAC is not yet covered by the literature.

The aim of this paper is thus to introduce a cooperative SLAC algorithm, where antenna responses and ranging biases are estimated during operation. We use a sensor fusion approach, utilizing the robot command velocity, gyroscope measurements and the received radio signals. The antenna response is represented in the state space using wavefield modeling and manifold separation. We introduce SLAC as an iterated extended Kalman filter (IEKF)-like Bayesian filtering algorithm. Then, we evaluate our proposed algorithm with measurement data obtained by software-defined radios (SDRs) mounted on robotic rovers. One rover is equipped with an MMA. We show that cooperative SLAC improves ranging and DoA performance, leading to better position and orientation accuracy.

II. Signal Model

Fig. 1 shows two agents i and j, which are part of the cooperative network, and the relevant metrics for 2D localization. Assuming RTT ranging, the distance between agents i and j

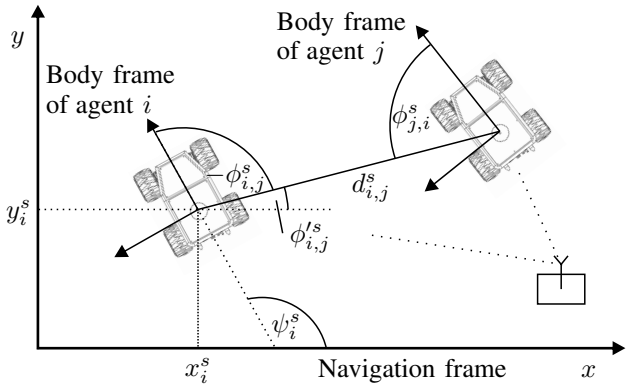

Fig. 1. Two agents i and j, the distance $d_{i,j}$ in between the agents, the DoAs $\phi_{i,j}$ and $\phi_{j,i}$ and the position $\boldsymbol{p}_i = [x_i \; y_i]^T$ and orientation ψ_i of agent i.

for snapshot s is defined as

$$d^s_{i,j} = \|\boldsymbol{p}^s_j - \boldsymbol{p}^s_i\| = \frac{c(\tau^s_{i,j} - \bar{\tau}^s_{i,j})}{2} + \delta^s_i + \delta^s_j, \tag{1}$$

where $\boldsymbol{p}^s_i = \begin{bmatrix} x^s_i & y^s_i \end{bmatrix}^T$ is the position of agent i, c is the speed of light, $\tau^s_{i,j}$ is the time-of-arrival (ToA) of the return signal, $\bar{\tau}^s_{i,j}$ is the transmit time of the forward signal and δ^s_i and δ^s_j are the ranging biases of agents i and j, respectively. We assume that the processing time at node j between receiving and transmitting back is very short and already compensated, such that the impact of the relative frequency offset of the clocks of agents i and j can be neglected. The signal DoA measured in the body frame of agent i is given by

$$\phi^s_{i,j} = \phi^{s\prime}_{i,j} - \psi^s_i = \operatorname{arctan2}\left(y^s_j - y^s_i,\, x^s_j - x^s_i\right) - \psi^s_i, \tag{2}$$

where ψ^s_i is the orientation of agent i in the navigation frame and $\operatorname{arctan2}(y, x)$ is the four-quadrant inverse tangent.

We assume that agent i receives a signal transmitted by agent j, which is sampled at rate B and a discrete Fourier transform (DFT) is performed. Following the narrowband assumption, the signal with snapshot index s is expressed as

$$\boldsymbol{r}^s_{i,j}(n) = \boldsymbol{a}_i(\phi^s_{i,j}) s(n, \tau^s_{i,j}) \alpha^s_{i,j}\, e^{\mathrm{j}\varphi^s_{i,j}} + \boldsymbol{w}^s_{i,j}(n), \tag{3}$$

with the index of the DFT bin $n \in \{1, ..., N\}$, the antenna response $\boldsymbol{a}_i(\phi^s_{i,j})$ of agent i, the amplitude of the signal $\alpha^s_{i,j}$ and the phase of the signal $\varphi^s_{i,j}$. A delayed version of the signal $s(n)$, transmitted by agent j, is given in discrete frequency domain by

$$s(n, \tau) = s(n) e^{-\mathrm{j}2\pi\tau B \frac{n-1}{N}}. \tag{4}$$

Receiver noise is taken into account by $\boldsymbol{w}^s_{i,j}(n) \sim \mathcal{CN}(0, \sigma^2_{\boldsymbol{r}^s_{i,j}} \mathbb{I}_M)$ as independent and identically distributed (i.i.d.) circular symmetric Gaussian noise with variance $\sigma^2_{\boldsymbol{r}^s_{i,j}}$. For each agent i, the antenna response

$$a_{i,m}(\phi) = \sqrt{g_{i,m}(\phi)} e^{\mathrm{j}\Phi_{i,m}(\phi)} \tag{5}$$

is described by the gain pattern $g_{i,m}(\phi)$ and phase pattern $\Phi_{i,m}(\phi)$ of the respective antenna port $m \in \{1, ..., M_i\}$, so we can define the antenna response vector as

$$\boldsymbol{a}_i(\phi) = \begin{bmatrix} a_1(\phi) & ... & a_{M_i}(\phi) \end{bmatrix}^T. \tag{6}$$

Agents with a singleport antenna, $M_i = 1$, are not capable of DoA estimation. Assuming half-wavelength dipoles, (6) simplifies accordingly to $a_i(\phi) = 10^{\frac{2.15\,\mathrm{dBi}}{20}}$. For signal processing, it is favorable that (6) can be expressed mathematically in closed-form. Such a representation is possible by wavefield modeling and manifold separation [7], [8], which allows us to decompose (6) as

$$\boldsymbol{a}_i(\phi) = \boldsymbol{G}_i\, \boldsymbol{b}(\phi). \tag{7}$$

$\boldsymbol{G}_i \in \mathbb{C}^{M \times U}$ is the sampling matrix, describing the antenna, and a $\boldsymbol{b}(\phi) \in \mathbb{C}^U$ is a basis vector, describing the wavefield or DoA. With the above representation, the SLAC algorithm proposed in this paper can be applied to arbitrary types of multiport antennas, e.g. phased arrays, co-located antennas or MMAs. A prerequisite for (7) is that the antenna response is square integrable and the chosen basis functions are orthonormal on the manifold $\phi \in [-\pi, \pi)$ [7], [8]. We use the Fourier functions

$$\boldsymbol{b}(\phi) = \frac{1}{\sqrt{2\pi}} e^{\mathrm{j}\phi u},\; u = \left\lfloor -\frac{U-1}{2} \right\rfloor, ..., 0, ..., \left\lfloor \frac{U-1}{2} \right\rfloor \tag{8}$$

as basis, where $\lfloor . \rfloor$ is the floor function. The order U of the basis functions is related to the electrical size of the antenna [7]. Wavefield modeling and manifold separation can be extended to azimuth and elevation using spherical harmonics or 2D Fourier functions as basis functions [7], [8], [1], which is beyond the scope of this paper.

When an antenna is measured, e.g. in a near-field measurement chamber, or an electromagnetic (EM) simulation is performed, spatial samples of (6) are obtained. Defining the sample index $q \in \{1, ..., Q\}$, the spatial samples obtained at DoAs ϕ_q are defined as $\boldsymbol{e}_q = \begin{bmatrix} e_{q,1} & ... & e_{q,M_i} \end{bmatrix}^T$ and $\boldsymbol{E}^0_i = \begin{bmatrix} \boldsymbol{e}_{i,1} & ... & \boldsymbol{e}_Q \end{bmatrix}^T$. Given that the spatial sampling grid fulfills the Nyquist condition, a sampling matrix can be obtained by

$$\boldsymbol{G}^0_i = \boldsymbol{E}^0_i \boldsymbol{B}^H (\boldsymbol{B}\boldsymbol{B}^H)^{-1}, \tag{9}$$

with $\boldsymbol{B} = [\boldsymbol{b}(\phi_1), ..., \boldsymbol{b}(\phi_Q)]$. However, EM simulation does not consider deviations during the antenna manufacturing. When the antenna alone is measured in a near-field measurement chamber, the influence of the platform, where the antenna is mounted, is neglected. Furthermore, the surrounding structure could be reconfigurable. The sampling matrix $\boldsymbol{G}^0_i$ from (9) will thus not be identical to the true sampling matrix $\boldsymbol{G}_i$, which impairs DoA estimation accuracy. In this paper, we thus propose a SLAC algorithm based on Bayesian filtering, which uses $\boldsymbol{G}^0_i$ as prior and estimates a refined sampling matrix over time.

III. State Space & Observation Model

The network consists of anchor nodes and $|\mathbb{A}|$ agent nodes, referred to by the agent set $\mathbb{A}$. Accordingly, the state vector is given by

$$\boldsymbol{x}^s = \begin{bmatrix} (\boldsymbol{x}^s_1)^T & ... & (\boldsymbol{x}^s_i)^T & ... & (\boldsymbol{x}^s_{|\mathbb{A}|})^T \end{bmatrix}^T, \tag{10}$$

with the state vector of agent i,

$$\boldsymbol{x}_i^s = \left[(\boldsymbol{x}_{i,\mathrm{loc}}^s)^T \quad (\boldsymbol{x}_{i,\mathrm{cal}}^s)^T\right]^T, \tag{11}$$

which contains the agent location states $\boldsymbol{x}_{i,\mathrm{loc}}^s$ and the agent calibration parameter states $\boldsymbol{x}_{i,\mathrm{cal}}^s$.

The location states of agent i are given by

$$\boldsymbol{x}_{i,\mathrm{loc}}^s = \left[(\boldsymbol{p}_i^s)^T \quad \psi_i^s\right]^T, \tag{12}$$

with position $\boldsymbol{p}_i^s$ and orientation ψ_i^s. The transition of the location states $\boldsymbol{x}_{i,\mathrm{loc}}^s$ of agent i from the previous snapshot $s^- = s-1$ to the current snapshot s is described by the robotic motion model

$$\boldsymbol{x}_{i,\mathrm{loc}}^s = \boldsymbol{f}(\boldsymbol{x}_{i,\mathrm{loc}}^{s^-}) + \boldsymbol{w}_{\boldsymbol{x}_{i,\mathrm{loc}}}^s, \tag{13}$$

$$\boldsymbol{f}(\boldsymbol{x}_{i,\mathrm{loc}}^{s^-}) = \begin{bmatrix} x_i^{s^-} \\ y_i^{s^-} \\ \psi_i^{s^-} \end{bmatrix} + \begin{bmatrix} -\frac{v_i^s}{\omega_i^s}\sin(\psi_i^{s^-}) + \frac{v_i^s}{\omega_i^s}\sin(\psi_i^{s^-} + \omega_i^s T) \\ \frac{v_i^s}{\omega_i^s}\cos(\psi_i^{s^-}) - \frac{v_i^s}{\omega_i^s}\cos(\psi_i^{s^-} + \omega_i^s T) \\ T\omega_i^s \end{bmatrix}, \tag{14}$$

from [9]. The model assumes control inputs of the turn rate ω_i^s and linear velocity v_i^s with additive Gaussian noise with variance σ_ω^2 and σ_v^2, respectively. On robotic platforms, ω_i^s and v_i^s are available by a gyroscope and the command velocity. The location process noise is $\boldsymbol{w}_{\boldsymbol{x}_{i,\mathrm{loc}}}^s \sim \mathcal{N}(\boldsymbol{0}_3, \boldsymbol{\Sigma}_{\boldsymbol{x}_{i,\mathrm{loc}}}^s)$, where the covariance $\boldsymbol{\Sigma}_{\boldsymbol{x}_{i,\mathrm{loc}}}^s$ is found by a transformation from control to state space [9].

The calibration states of agent i are given by

$$\boldsymbol{x}_{i,\mathrm{cal}}^s = \left[\delta_i^s \quad (\boldsymbol{g}_i^s)^T\right]^T, \tag{15}$$

with the ranging bias δ_i^s and the vectorized sampling matrix entries split into real and imaginary part,

$$\boldsymbol{g}_i^s = \begin{bmatrix} \mathrm{Re}\left\{\mathrm{vec}\left\{\boldsymbol{G}_i^s\right\}\right\} \\ \mathrm{Im}\left\{\mathrm{vec}\left\{\boldsymbol{G}_i^s\right\}\right\} \end{bmatrix}, \tag{16}$$

which only exist for multiport agents $M_i > 1$. The operator $\boldsymbol{a} = \mathrm{vec}\left\{\boldsymbol{A}\right\}$ vectorizes matrix $\boldsymbol{A}$ by stacking its columns. The calibration parameters $\boldsymbol{x}_{i,\mathrm{cal}}^s$ are assumed to be constant over time with zero process noise.

A common approach to cooperative localization is to first estimate the agent distances and relative directions. In a second step, agent positions and orientations are estimated by a subsequent algorithm. Contrarily, for cooperative SLAC we need to use the received signals directly as observations, otherwise the antenna response is not observable. The observations vector is thus

$$\boldsymbol{z}^s = \left[\ldots \quad (\boldsymbol{r}_{i,j}^s)^T \quad \ldots \quad (\boldsymbol{r}_{j,i}^s)^T \quad \ldots\right]^T. \tag{17}$$

The observation model is given by the concentrated log-likelihood functions, where the unknown signal amplitude $\alpha_{i,j}^s$ and phase $\varphi_{i,j}^s$ have been eliminated. Defining $\boldsymbol{r}_{i,j}^s = \left[(\boldsymbol{r}_{i,j}^s(1))^T, \ldots, (\boldsymbol{r}_{i,j}^s(N))^T\right]^T$, the concentrated log-likelihood function for agents with a multiport antenna, $M_i > 1$, is given by

$$\tilde{L}(\boldsymbol{r}_{i,j}^s | \phi_{i,j}^s, \tau_{i,j}^s, \boldsymbol{g}_i^s) = \frac{1}{\sigma_{\boldsymbol{r}_{i,j}^s}^2} \left\| \frac{\boldsymbol{e}_{i,j}^s (\boldsymbol{e}_{i,j}^s)^H}{(\boldsymbol{e}_{i,j}^s)^H \boldsymbol{e}_{i,j}^s} \boldsymbol{r}_{i,j}^s \right\|^2 \tag{18}$$

according to [10], where we define the vectors $\boldsymbol{e}_{i,j}^s = \mathrm{vec}\left\{\boldsymbol{a}(\phi_{i,j}^s)\boldsymbol{s}^T(\tau_{i,j}^s)\right\}$ and $\boldsymbol{s}(\tau_{i,j}^s) = \left[s(1,\tau_{i,j}^s), \ldots, s(N,\tau_{i,j}^s)\right]^T$. For agents with a singleport antenna, $M_i = 1$, (18) simplifies to

$$\tilde{L}(\boldsymbol{r}_{i,j}^s | \tau_{i,j}^s) = \frac{1}{\sigma_{\boldsymbol{r}_{i,j}^s}^2} \frac{\left|\boldsymbol{s}^H(\tau_{i,j}^s)\boldsymbol{r}_{i,j}^s\right|^2}{\left\|\boldsymbol{s}(\tau_{i,j}^s)\right\|^2}. \tag{19}$$

The noise variance $\sigma_{\boldsymbol{r}_{i,j}^s}^2$ in (18) and (19) is estimated based on the known transmitted signal.

IV. SLAC Algorithm

We propose to implement cooperative SLAC as a Bayesian filtering algorithm, where the posterior probability density function (pdf) is calculated recursively by prediction and update steps [9], [11]. The measurement models (18) and (19) are highly nonlinear, thus applying linearization as in the extended Kalman filter (EKF) is unfavorable. Furthermore, the state vector (10) has high dimensionality, as it contains the entries of the sampling matrix $\boldsymbol{G}^s$. High state dimensionality is challenging for sampling-based approaches like particle filtering. As a consequence, we propose to use the IEKF [11] with Laplace approximation for the covariance update [12]. The IEKF assumes that the pdfs are Gaussian distributed and can thus be described by their mean and covariance.

Prediction of the location states is done according to the motion model (14),

$$\bar{\boldsymbol{x}}_{i,\mathrm{loc}}^s = \boldsymbol{f}(\hat{\boldsymbol{x}}_{i,\mathrm{loc}}^{s^-}) \quad \forall\, i \in \mathbb{A}, \tag{20}$$

where $\hat{\boldsymbol{x}}_{i,\mathrm{loc}}^{s^-}$ are the estimated location states of the previous snapshot. The calibration parameter states remain constant. As in the EKF, the predicted covariance is

$$\bar{\boldsymbol{\Sigma}}^s = \boldsymbol{F}^{s^-} \hat{\boldsymbol{\Sigma}}^{s^-} (\boldsymbol{F}^{s^-})^T + \boldsymbol{\Sigma}_{\boldsymbol{x}}^s, \tag{21}$$

where $\hat{\boldsymbol{\Sigma}}^{s^-}$ is the estimated covariance matrix of the previous snapshot. The entries of the Jacobian matrix $\boldsymbol{F}^{s^-}$ related to the location states are given by the Jacobian matrix of the robotic motion model (14), see [9]. The diagonal entries of $\boldsymbol{F}^{s^-}$ related to the calibration states consist of ones, the off-diagonal elements of zeros. $\boldsymbol{\Sigma}_{\boldsymbol{x}}^s$ is the process noise covariance matrix, which is composed of $\boldsymbol{\Sigma}_{\boldsymbol{x}_{i,\mathrm{loc}}}^s$ for the location states and ones on the diagonal for the calibration states.

Following the IEKF, which uses a maximum a posteriori (MAP) approach, the updated state estimate is

$$\hat{\boldsymbol{x}}^s = \arg\max_{\boldsymbol{x}^s} \underbrace{L\left(\boldsymbol{z}^s | \boldsymbol{x}^s\right) + L\left(\boldsymbol{x}^s | \boldsymbol{z}^{1:s^-}\right)}_{g(\boldsymbol{x}^s)}, \tag{22}$$

where we assume independent process noise for the agents and independent measurement noise for the signals received by the agents. The Gaussian prior from the previous snapshot is given by

$$L\left(\boldsymbol{x}^s | \boldsymbol{z}^{1:s^-}\right) = \frac{1}{2}(\boldsymbol{x}^s - \bar{\boldsymbol{x}}^s)^T \left(\bar{\boldsymbol{\Sigma}}^s\right)^{-1} (\boldsymbol{x}^s - \bar{\boldsymbol{x}}^s). \tag{23}$$

The log-likelihood of the observations is a double sum over all received signals,

$$L\left(\boldsymbol{z}^s|\boldsymbol{x}^s\right) = \sum_{i\in\mathbb{A}} L\left(\boldsymbol{z}_i^s|\boldsymbol{x}_i^s\right) = \sum_{i\in\mathbb{A}}\sum_{j\in\mathbb{L}_i^s} L\left(\boldsymbol{r}_{i,j}^s|\boldsymbol{x}_i^s,\boldsymbol{x}_j^s\right), \quad (24)$$

where the set $\mathbb{L}_i^s$ contains the neighboring agents and anchors, from which agent i has received signals with snapshot index s. The log-likelihoods are given by (19) and (18) for receiving singleport and multiport antennas:

$$L\left(\boldsymbol{r}_{i,j}^s|\boldsymbol{x}_i^s,\boldsymbol{x}_j^s\right) = \begin{cases} \tilde{L}\left(\boldsymbol{r}_{i,j}^s|\phi_{i,j}^s,\tau_{i,j}^s,\boldsymbol{g}_i^s\right), & \text{if } M_i > 1 \\ \tilde{L}\left(\boldsymbol{r}_{i,j}^s|\tau_{i,j}^s\right), & \text{if } M_i = 1. \end{cases} \quad (25)$$

A solution to (22) is obtained by the quasi-Newton Broyden–Fletcher–Goldfarb–Shanno (BFGS) algorithm, using the gradient

$$\nabla \boldsymbol{g}(\boldsymbol{x}^s) = \sum_{i\in\mathbb{A}}\sum_{j\in\mathbb{L}_i^s} \frac{\partial L\left(\boldsymbol{r}_{i,j}^s|\boldsymbol{x}_i^s,\boldsymbol{x}_j^s\right)}{\partial \boldsymbol{x}^s} + \left(\bar{\boldsymbol{\Sigma}}^s\right)^{-1}\left(\boldsymbol{x}^s - \bar{\boldsymbol{x}}^s\right). \quad (26)$$

As prediction based on control inputs is used in (14), the predicted state $\bar{\boldsymbol{x}}^s$ is close to the solution $\hat{\boldsymbol{x}}^s$, ensuring fast convergence of the algorithm. The updated covariance matrix is calculated numerically by the inverse of the Hessian matrix at the solution, which is called Laplace approximation [12].

At snapshot $s = 0$, the Bayesian filtering algorithm is initialized. An initial estimate of the agent positions $\boldsymbol{p}_i^0 = \left[x_i^0, y_i^0\right]^T$ and orientations ψ_i^0 can be obtained by a snapshot-based position and orientation estimation algorithm, see e.g. [13]. The ranging bias is expected to be small, so it is initialized with $\delta_i^0 = 0\,\mathrm{m}$. For the sampling matrix entries $\boldsymbol{g}_i^0$, prior knowledge is available from an EM simulation or from measuring the antenna in a near-field measurement chamber.

V. Measurements Results

The measurement scenario is shown in Fig. 2 and consists of three anchor nodes A1, A2, A3 and four robotic agents Dias, Drake, Magellan, Vespucci. The robotic agents are Robotnik Summit XL rovers with skid-steering. Due to skid, the command angular velocity is not reliable. We thus use the command linear velocity and gyroscope measurements as control inputs for the motion model (14). The anchor nodes and the agents Drake, Magellan and Vespucci are equipped with dipole antennas and Ettus Research Universal Software Radio Peripheral (USRP) B200mini SDRs. Dias is equipped with a four-port MMA and a USRP N310. The local oscillator (LO) for the N310 is provided by an external frequency synthesizer. Phase and amplitude imbalances between the four channels are compensated, enabling phase-coherent reception. The in-house developed MMA is a dielectric resonator antenna with four independently excited modes [14], which is suitable for DoA estimation [1]. The physical layer is based on the DLR Swarm Communication and Navigation system [15]. For this experiment, the transmit power is $-15\,\mathrm{dBm}$, the carrier frequency is 1.68 GHz, the occupied bandwidth is approx. 28.2 MHz and we use orthogonal frequency-division multiplexing (OFDM) with fast Fourier transform (FFT) length 1024. For the manifold separation (7), $U = 13$ basis functions (8) are chosen to represent the antenna response. The experiment duration was 12 min 30 s. For the first part, only Dias (MMA) was driving until 6 min 0 s, when also Drake and Vespucci started driving. Magellan remained static. The signals received by all nodes have been stored and evaluated by post-processing. The update interval is $T = 0.1\,\mathrm{s}$ and the control input noise parameters are assumed to be $\sigma_v = 0.015\,\mathrm{m/s^{1.5}}$ and $\sigma_\omega = 0.3\,^\circ/\mathrm{s}^{1.5}$. For localization-only, we use the same algorithm as for SLAC, outlined in Section IV, but the calibration states (15) are omitted from the state space. Ground-truth for the positions and orientations of the agents is provided by a commercial dual antenna real-time kinematic (RTK) system.

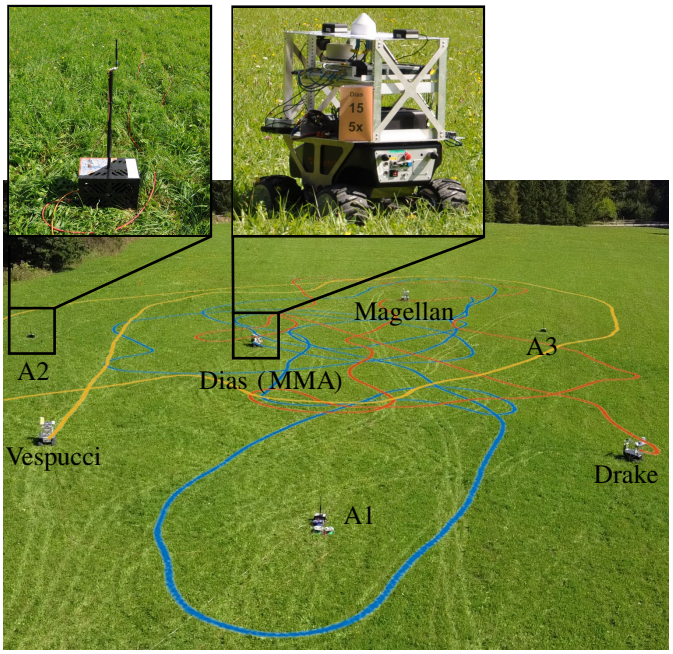

Fig. 2. Measurement scenario with anchor nodes A1, A2, A3 and robotic agents Dias (MMA), Drake, Magellan, Vespucci. Agent trajectories are plotted in blue (Dias), orange (Drake) and yellow (Vespucci). Magellan is static.

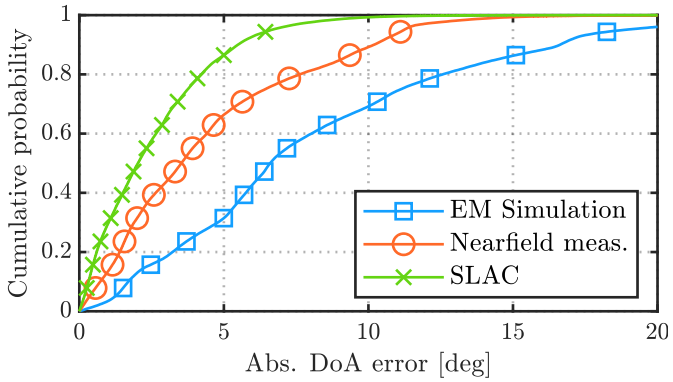

Fig. 3. Empirical CDF of the absolute DoA estimation error, for all signals received by agent Dias. DoA estimation is performed using the antenna response from EM simulation, from a near-field measurement or by SLAC.

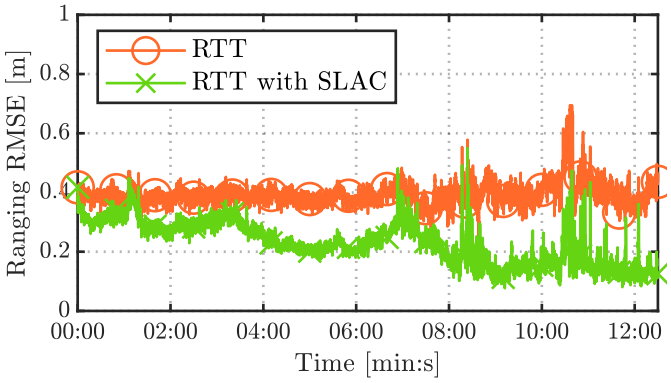

Fig. 4. Ranging RMSE, calculated over all links in the network, without correction and with SLAC.

TABLE I
POSITION AND ORIENTATION RMSES.

Rover	Position RMSE Loc.	Position RMSE SLAC	Orient. RMSE Loc.	Orient. RMSE SLAC
Dias (MMA)	0.32 m	0.26 m	2.1°	1.8°
Drake	0.68 m	0.40 m	8.5°	7.9°
Vespucci	0.72 m	0.44 m	6.6°	6.4°
Magellan (static)	0.36 m	0.30 m	6.6°	6.6°

To evaluate the antenna response calibration by SLAC, we have performed DoA estimation for the signals received by rover Dias in post-processing by a coherent maximum likelihood (ML) estimator [1]. Fig. 3 shows the resulting empirical cumulative distribution function (CDF) curves of the absolute DoA estimation error, where three different antenna responses have been assumed. The three antenna responses are obtained by EM simulation, by measuring the antenna in a StarLab near-field measurement system, and by SLAC. The 90$^{\text{th}}$ percentile DoA estimation errors are given by 16.6°, 10.2° and 5.6° for the respective antenna response. Thus, SLAC is able to correctly estimate the antenna response during operation.

Fig. 4 shows the ranging root-mean-square error (RMSE), i.e. the RMSE of the estimated ranges (1) calculated over all links in the network, without ranging bias correction and with SLAC, respectively. Without ranging bias correction, the ranging RMSE is mostly around 0.4 m except for several spikes towards the end of the measurement, due to larger distances between the nodes. With SLAC, the ranging RMSE decreases below 0.4 m, as the ranging biases of the nodes are estimated over time. The ranging RMSE with SLAC is strictly smaller than without ranging bias correction, which highlights the benefit of estimating ranging biases during localization.

Ultimately, position and orientation RMSE are important figures to determine localization accuracy. Table I shows the position and orientation RMSEs for both, localization-only and SLAC. Using SLAC yields lower position and orientation RMSEs for all agents except Magellan. As Magellan remained static, its orientation accuracy could not be improved.

VI. CONCLUSION

In this paper, we have introduced calibration of antenna responses and ranging biases simultaneously with localization, called SLAC. By measurement data from SDRs installed on four robotic rovers, one capable of DoA estimation, we have demonstrated the feasibility of the proposed approach. We have shown that SLAC is able to estimate ranging biases, leading to a reduced ranging RMSE. Furthermore, we have demonstrated that DoA estimation performance is improved by SLAC, indicating correct estimation of the antenna response. Finally, we have shown that SLAC improves the position and orientation accuracy in a realistic scenario.

REFERENCES

[1] R. Pöhlmann, S. A. Almasri, S. Zhang, T. Jost, A. Dammann, and P. A. Hoeher, "On the potential of multi-mode antennas for direction-of-arrival estimation," *IEEE Transactions on Antennas and Propagation*, vol. 67, no. 5, pp. 3374–3386, May 2019.

[2] R. Pöhlmann, E. Staudinger, S. Zhang, S. Caizzone, A. Dammann, and P. A. Hoeher, "In-field calibration of a multi-mode antenna for DoA estimation," in *Proc. 15th European Conf. Antennas and Propagation (EuCAP)*, Mar. 2021.

[3] C. Cadena, L. Carlone, H. Carrillo, Y. Latif, D. Scaramuzza, J. Neira, I. Reid, and J. J. Leonard, "Past, present, and future of simultaneous localization and mapping: Toward the robust-perception age," *IEEE Transactions on Robotics*, vol. 32, no. 6, pp. 1309–1332, Dec. 2016.

[4] H. Sadjadi, K. Hashtrudi-Zaad, and G. Fichtinger, "Simultaneous localization and calibration for electromagnetic tracking systems," *The International Journal of Medical Robotics and Computer Assisted Surgery*, vol. 12, no. 2, pp. 189–198, Jun. 2016.

[5] C. Taylor, A. Rahimi, J. Bachrach, H. Shrobe, and A. Grue, "Simultaneous localization, calibration, and tracking in an ad hoc sensor network," in *Proc. 5th Int. Conf. Information Processing in Sensor Networks*, Nashville, Tennessee, Apr. 2006, pp. 27–33.

[6] N. Petrov, O. Krasnov, and A. G. Yarovoy, "Auto-calibration of automotive radars in operational mode using simultaneous localisation and mapping," *IEEE Transactions on Vehicular Technology*, vol. 70, no. 3, pp. 2062–2075, Mar. 2021.

[7] M. A. Doron and E. Doron, "Wavefield modeling and array processing. I. Spatial sampling," *IEEE Transactions on Signal Processing*, vol. 42, no. 10, pp. 2549–2559, Oct. 1994.

[8] M. Costa, A. Richter, and V. Koivunen, "Unified array manifold decomposition based on spherical harmonics and 2-D fourier basis," *IEEE Transactions on Signal Processing*, vol. 58, no. 9, pp. 4634–4645, Sep. 2010.

[9] S. Thrun, W. Burgard, and D. Fox, *Probabilistic Robotics*. MIT Press, Aug. 2005.

[10] M. Wax and A. Leshem, "Joint estimation of time delays and directions of arrival of multiple reflections of a known signal," *IEEE Transactions on Signal Processing*, vol. 45, no. 10, pp. 2477–2484, Oct. 1997.

[11] Y. Bar-Shalom, X. R. Li, and T. Kirubarajan, *Estimation with Applications to Tracking and Navigation: Theory Algorithms and Software*. John Wiley & Sons, 2004.

[12] L. Tierney and J. B. Kadane, "Accurate approximations for posterior moments and marginal densities," *Journal of the American Statistical Association*, vol. 81, no. 393, pp. 82–86, Mar. 1986.

[13] H. Naseri and V. Koivunen, "A Bayesian algorithm for distributed cooperative localization using distance and direction estimates," *IEEE Transactions on Signal and Information Processing over Networks*, pp. 290–304, Nov. 2018.

[14] S. Caizzone, M. S. Circiu, W. Elmarissi, and C. Enneking, "All-GNSS-band DRA antenna for high-precision applications," in *Proc. 12th European Conf. Antennas and Propagation (EuCAP)*, Apr. 2018, pp. 543–547.

[15] S. Zhang, R. Pöhlmann, E. Staudinger, and A. Dammann, "Assembling a swarm navigation system: Communication, localization, sensing and control," in *Proc. 1st IEEE Int. Workshop Communication and Networking for Swarms Robotics (RoboCom)*, Online, Jan. 2021.